The mixed impact of nanoclays on the apparent diffusion coefficient of additives in biodegradable polymers in contact with food

Anais Lajarrige, Nathalie Gontard, Sebastien Gaucel, Marie-Francoise Samson, Stéphane Peyron

The mixed impact of nanoclays on the apparent diffusion coefficient of additives in biodegradable polymers in contact with food

Anaïs Lajarrige[a]*, Nathalie Gontard[a], Sébastien Gaucel[a], Marie-Françoise Samson[a] and Stéphane Peyron[a]

[a]JRU IATE 1208, CIRAD, INRA, Montpellier SupAgro, University of Montpellier, 2 place Pierre Viala, F-34060 Montpellier 01, France

nathalie.gontard@inra.fr

sebastien.gaucel@inra.fr

marie-francoise.samson@inra.fr

stephane.peyron@univ-montp2.fr

*Corresponding author: E-mail adress: lajarrige.anais@hotmail.fr

Abstract

In face of growing environmental concerns, biodegradable and bio-sourced plastic nanocomposites are emerging as a new class of materials, especially for the food packaging sector. However, their use in food contact raises new issues in term of consumer safety.

The aim of this study was to determine the impact of nanoclays on the apparent diffusion coefficient (D_{app}) of selected additives from biopolymers into fatty food simulants. For the most part, nanoclay addition has a non-conventional impact. To understand this, the following parameters were studied: (i) the exfoliation state of nanoclay platelets in the polymer matrix, (ii) the sorption of food simulant by the polymer matrix, and (iii) the crystallinity of the materials. At first glance, solvent uptake and crystallinity agree with the results of diffusivity, however these parameters cannot explain the extreme differences between D_{app} values.

Keywords: nanoclays, biopolymer, apparent diffusion coefficient (D_{app}), additives, food packaging

1 Introduction

The growing global production and consumption of plastic materials engenders serious environmental concerns (Kirwan and Strawbridge, 2003), primarily the need to implement eco-efficient end-of-life treatments. For many years, alternative materials based on bio-sourced and biodegradable polymers have been considered as innovative and promising materials for future food packaging applications (Tharanathan, 2003; Sorrentino et al., 2007). However, the substitution of plastic in all its various uses in food packaging remains difficult given the broad spectrum of functionality offered by petroleum-based polymers. In addition to their high water sensitivity, the properties of biodegradable materials make them uncompetitive in comparison with those of conventional plastic polymers, particularly in terms of barrier properties. The addition of reinforcing fillers such as clay nanoparticles, giving rise to the formation of a bio-nanocomposite material, is widely considered as the solution to this problem (Perumal et al., 2018).

The introduction of nanotechnologies to the field of food packaging raises new issues related to consumer safety. Research has focused on the exposure of consumers to nanoparticles through contamination of the food in contact with nanocomposite materials. There is a consensus in the research on the migration of nanoclay that its limited diffusion under a nanoform in a polymeric matrix prevents its migration into food (Šimon et al., 2008). Like any material in contact with food, nano- and bio-nanocomposite materials are subject to the European framework regulation UE 1935/2004. In the absence of specific regulations covering their use in contact with food, the suitability for food contact applications of nanocomposite packaging are assessed according to the recommendations established for plastic materials specified in the regulation EU/10/2011.

Given the impact of nanoclays on the transfer properties of materials (Muñoz-Shugulí et al., 2019), it is logical to investigate their impact on the migration of property-enhancing

plastics additives such as plasticizers, UV-stabilizers, anti-oxidants, and anti-static agents (Figge, 1980). The impact of nanoparticles on the potential migration of low molar mass additives has received little attention, the only studies having focused on plastic-based nanocomposite materials. These studies, performed on nanocomposite materials, specifically: PETs (Farhoodi et al., 2016), polyamides (Pereira de Abreu et al., 2010), and polyolefins (Otero-Pazos et al. 2016; Nasiri et al. 2016; Nasiri et al. 2017), conclude that nanoparticles decrease the diffusivity of low molar mass substances. Such results suggest the applicability of the Piringer model in a migration prediction approach based on an overestimated value of diffusivity.

From a safety standpoint, the barrier effect provided by the nanostructure of packaging film against additives could reduce the exposure of consumers to toxic compounds and their potential adverse health effects, depending on the individual barrier properties of polymers. Although nanoclays have a positive effect on high barrier polymers such as PET, the decrease in the diffusion coefficient has no effect on the migration value for low-barrier polymers, for which the migration values are more related to the partition coefficient (Farhoodi et al., 2016). The reasons why the presence of nanoparticles decreases the mobility of the diffusing molecules are multiple. While the tortuosity effect is generally cited (Paul and Robeson, 2008; Duncan, 2011), the mechanisms of diffusion in nanocomposite matrices imply additional essential factors. In the case of polymer-clay nanocomposites, the interactions of organic molecules with the clay's minerals are likely to generate a decrease in their D_{app} by sorption or adsorption mechanisms (Nasiri et al. 2016). In addition to their high cation exchange capacity, clays can exchange other chemical bonds, such as van der Walls interactions, or hydrogen bonding, with migrants, delaying their transport in the nanocomposite structure (Aguzzi et al., 2007). It is also well established that the presence of clay nanoparticles structurally modifies polymer networks, having nucleating effects, and their ability to increase the crystallization rate of semi-crystalline

thermoplastic polymers (Ke et al., 1999; Yuan et al., 2006). At a finer scale, crystallinity gradients in the vicinity of nanoparticles can have a modulating effect on the transfer properties of plastic-based nanocomposites (Wurm et al., 2010). This combination of effects emphasized nanocomposite bioplastics (Charlon et al. 2015b), but to our knowledge, no research has measured and characterized migration from bio-nanocomposite packaging. Such materials, by definition unstable, may behave differently than synthetic polymers in contact with food, and their inertial properties remain undemonstrated. This study aims to characterize the food contact suitability of bio-nanocomposite packaging films. In view of their emergence on the market and their environmental benefits (Rajan et al., 2018; Hongsriphan and Pinpueng, 2019), two distinct polymers: poly(butylene succinate-co-butylene adipate) (PBSA) and poly(hydroxybutyrate-co-hydroxyvalerate) (PHBV) were selected on the basis of their differing transfer properties, in order to cover different behaviors in contact with food simulants, the PHBV being a high-barrier polymer (Crétois et al., 2014) contrary to PBSA (Phua et al., 2013). Organo-modified montmorillonite was added to these materials, which were spiked with a panel of target migrating substances and submitted to migration tests following the protocol for testing conventional plastic packaging. The approach aims to measure and identify the influence of nanoclays on the diffusion properties of these emerging packaging materials.

2 Materials and Methods

2.1 Materials

Poly(butylene succinate-co-butylene adipate) (PBSA, PBE 001, density 1.24 g.cm^{-3}) and Poly(hydroxybutyrate-co-hydroxyvalerate) (PHBV, PHI 002, density 1.23 g.cm^{-3}) pellets were commercially procured from Natureplast, France.

Cloisite 30B (C-30B), an organo-modified montmorillonite clay containing a methyl bis-2-hydroxyethyl ammonium quaternary salt with a cation exchange capacity (CEC) of 90

meq/100 g, were supplied by BYK additives & instruments, Germany. C-30B was chosen because of its favorable interaction with PBSA (Sinha Ray et al., 2008) and PHBV (Carli et al., 2011; Iggui et al., 2015).

An array of solid and liquid additives was chosen. These molecules represent a range of categories of chemical compounds with a variety of chemical and physical properties as described in FDA and EFSA regulations (Food and Drug Administration, 2006; European Food Safety Authority, 2011). The additives chosen include: volatile polar organic substances, volatile non-polar organic substances, non-volatile polar organic substances, and non-volatile non-polar organic substances. Three high molar mass additives and eight low molar mass additives were procured from Sigma-Aldrich (Table 1).

2.2 Preparation of bio-nanocomposite films

PBSA and PHBV films with 5 wt% C-30B were synthetized by a melt extrusion process using an EuroLab 16XL co-rotating twin-screw extruder (Thermo Scientific^{TM}, Germany) with a L/D ratio of 40 and a screw diameter of 16 mm. The extruder produced films using a calendar die. Polymer pellets were dried at 60°C for 15 hours before use to remove residual moisture. Nanoclays were used without drying, because hydrated nanoclay platelets intercalate better with the polymer matrix (Tenn et al., 2013).

PBSA films were produced in three stages (Charlon et al. 2015a). First, a masterbatch of 15 wt% C-30B was prepared. The polymer pellets and nanoclays were introduced in the extruder at a flow rate of 0.85 $kg.h^{-1}$ and 0.15 $kg.h^{-1}$, respectively. The feed to die temperature profile was 120°C to 160°C. At the extrusion die, the emerging polymers were cooled in a water bath and pelletized. The masterbatch was then diluted with neat polymer to obtain 5 wt% nanoclay pellets. Finally, films of 180 ± 10 µm for PBSA and 220 ± 25 µm for PBSA nanocomposite (PBSA NCP) were produced from these pellets using a flow rate of 1.0 $kg.h^{-1}$

and a 100°C to 135°C temperature profile. All steps were processed at a screw speed of 200 rpm.

PHBV films were produced in two stages (Iggui et al., 2015). A masterbatch of 15 wt% C-30B was prepared in the same way as for PBSA, however with a temperature profile of 140°C to 180°C. The masterbatch was diluted with neat polymer to obtain PHBV films containing 5 wt% nanoclay. The films of 145 ± 20 µm for PHBV and 140 ± 10 µm for PHBV NCP were produced using a screw speed of 210 rpm and a flow rate of 1.0 $kg.h^{-1}$. PBSA and PHBV pellets or films were oven dried at 60°C for 15 hours after each stage and before storage.

The control samples of neat PBSA and PHBV were prepared following the same protocol used for nanocomposites in order to respect the same thermal processes.

2.3 Spiking of neat and nanocomposite films

The procedure used for the spiking of films depends on additive molar mass. High molar mass additives were introduced to films during the extrusion process because of their excellent thermal stability (Mauricio Iglesias, 2009). The theoretical additive amount was 500 ppm. Low molar mass additives were introduced to films through contamination at 40°C for 7 days under rotary agitation. The theoretical additive amount was 500 ppm for all low molar mass additives apart from toluene at 1000 ppm.

2.4 Food simulants

Two different food simulants were chosen to evaluate the D_{app} of the selected additives: 95% ethanol, and iso-octane, which both simulate fatty foods behaviors according to the European Commission for food contact materials (EU 10/2011) (Commission, 2011). The experiments were also performed using 3% acetic acid to simulate acidic food behavior, but the migration of high molar mass additives in this solvent was less than the limit of detection.

2.5 Desorption tests

Desorption tests were carried out by putting contaminated films in contact with food simulants in a surface/volume ratio of 6 $dm^2.L^{-1}$. The bottles were stored under magnetic agitation at 40°C for 10 days, except for PHBV films contaminated by high molar mass additives, for which storage was increased to 30 days. Over specific periods of time, an aliquot of each food simulant was collected and analyzed by chromatography (GC-FID for low molar mass additives or HPLC for high molar mass additives). The samples of iso-octane were evaporated under nitrogen and re-dissolved in 100% ethanol before HPLC analysis.

2.6 Small angle X-ray diffraction (SAXS)

SAXS experiments were performed using an "in-house" setup to study the degree of exfoliation of the nanoclays in the polymer matrix. A high brightness low power X-ray tube, coupled with aspheric multilayer optic (GeniX^{3D} from Xenocs) delivered an ultralow divergent beam (0.5 mrad; flux: 20 MPhotons.s^{1}; λ = 1.5418 Å; size at sample: 0.6*0.6 mm). A transmission configuration was used and the scattered intensity determined by a 2D pixel "Pilatus" detector at a distance of 1.9 m from the sample. Glass capillary support was used in the case of nanoclay powder, while for films, the beam passed through five stacked film thicknesses. The obtained intensities were corrected by transmission and the empty cell contribution was subtracted. The interlayer spacing relative to nanoclay platelets was determined at a diffraction angle in the range of 0.5° to 10°.

2.7 Transmission electron microscopy (TEM)

A JEOL 1200EX2 transmission electron microscope with 100 kV acceleration voltage equipped with an EMSIS Olympus camera was used to analyze film samples and observe

nanoclay dispersion and exfoliation in the polymer matrix. For that, the film samples were included in a resin and cut with a Leica UC 7 ultramicrotome.

2.8 Differential scanning calorimetry (DSC)

A differential scanning calorimeter (DSC series Q200, TA Instruments) was used to study the crystallinity of the films. Experiments were carried out on neat and nanocomposite films, before and after 10 days of contact with 95% ethanol or iso-octane. All measurements were performed under a nitrogen atmosphere. Specimens of 5-8 mg, weighed using a microbalance (Sartorius micro PRO 11), were placed in aluminum sample pans. The thermal protocol was defined according to the polymer. The PBSA samples were: heated from ambient temperature to 40°C, cooled to - 35°C, heated to 150°C, maintained at 150°C for 5 min, cooled to - 35°C, heated to 150°C, and finally cooled to 40°C. In the case of PHBV, samples were: heated from ambient temperature to 40°C, cooled to - 30°C, heated to 200°C, maintained at 200°C for 5 min, cooled to - 30°C, reheated to 200°C, and finally cooled to 40°C. Temperatures were adjusted at a rate of 10°C.min^{-1}. The apparent melting enthalpy (ΔHm) was determined from the DSC curves using the Universal Analysis 2000 software by TA Instruments. The crystallinity degree (X_C) of neat and nanocomposite polymers was determined by the equation:

$$X_C(\%) = \frac{\Delta H_m}{\Delta H_m^0} \times \frac{100}{w} \quad (1)$$

Where: ΔHm is the melting enthalpy of the polymer matrix, w is the polymer weight fraction in the sample and ΔH_m^0 is the theoretical melting enthalpy of the polymer assumed to be 100% crystalline, ΔH_m^0 = 146.0 J.g^{-1} for PHBV (Barham et al., 1984) and ΔH_m^0 = 116.9 J.g^{-1} for PBSA (Nikolic and Djonlagic, 2001).

2.9 Sorption of food simulants

The food simulant uptake by the films was determined by gravimetric measurements using a precision balance (10^{-4} g) before and after subjecting films to contact with food simulants at 40°C for 10 days under magnetic agitation. At the end of this procedure, excess food simulant was removed with tissue paper before re-measuring. The percentage of solvent uptake was obtained by the following equation:

$$\text{Sorption} = \frac{m_t - m_i}{m_i} \times 100 \quad (2)$$

Where: m_i and m_t are weights of samples before and after sorption, respectively.

2.10 Gas chromatography with flame ionization detector (GC-FID)

An Agilent 7890A GC equipped with a 7693A Automatic Sampler and a flame ionization detector was used to determine the concentration of low molar mass additives (< 400 $g.mol^{-1}$) in food simulants. The components were separated using a HP-5 (5%-phenyl)methylpolysiloxane capillary column of 32 mm ID and 30 m length. The thermal protocol used for the oven was as follows: an initial temperature of 40°C maintained for 5 min, heated at a rate of 6°C.min^{-1} to 270°C, maintained for 15 min. The injector temperature was 250°C. An external calibration was made in each food simulant in the range of 1.25 – 40 $mg.L^{-1}$.

2.11 High performance liquid chromatography (HPLC)

An Alliance HPLC system (Waters) equipped with an Alltima C18 column (250 mm × 2.1 mm, 5-µm) protected with a Alltima C18 (7.5mm × 2.1 mm, 5-µm) column guard was used to determine the concentration of high molar mass additives in food simulants. Compounds were separated with 55% acetonitrile at a flow rate of 0.3 mL.min^{-1} at 50°C. Absorbance was

recorded at 230 nm to quantify the additive concentration. An external calibration was made in each food simulant with concentrations of 1.25 to 20 $mg.L^{-1}$.

2.12 Estimation of the D_{app}

2.12.1 Fick's second diffusion equation

The D_{app} of additives from the polymer films into food simulant was calculated from experimental desorption kinetic curves using Fick's second law. The films are considered as one-dimensional infinite plane sheets, given that diffusion via the borders of the films is negligible. Applying Fick's second law results in the following one dimensional diffusion equation:

$$\frac{\partial C}{\partial t} = D_{app}\left(\frac{\partial^2 C}{\partial x^2}\right) \quad (3)$$

Where: C is the additive concentration, t, the contact time, x, the position in the film and D_{app}, the apparent diffusion coefficient.

The Eq. (3) was solved using the following initial (Eq. 4) and boundary (Eq. 5) conditions:

$$C(t = 0, x) = C_0 \; \forall \, x \in [-L, L] \quad (4)$$

$$C(t, x = \pm L) = C_s(t) \; \forall \, t \geq 0 \quad (5)$$

Where: $C_s(t)$ is the additive concentration in food simulant at time t and L, the film half thickness.

This diffusion model can be used provided that the following assumptions are verified (Helmroth et al., 2002): (i) additive contamination of the film is homogeneous, (ii) there is no noticeable swelling caused by interaction between the food simulant and the polymer, (iii) there is no concentration gradient in the food simulant, and (iv) the film thickness is homogeneous. In the case of an infinite plane sheet suspended in a stirred solution of limited volume, the Eq. (3) can be solved analytically as described by Crank (Crank, 1975):

$$\frac{M_t}{M_\infty} = 1 - \sum_{n=0}^{\infty} \frac{2\,\alpha\,(1+\alpha)}{1+\alpha+\alpha^2\,q_n^2} \exp\left\{-\frac{D\,q_n^2\,t}{L^2}\right\} \quad (6)$$

With:

$$\alpha = \frac{1}{K_{P,F}} \frac{V_F}{V_P} \quad (7)$$

Where: Mt is the total amount of additives in food simulant at time t and M_∞ is the total amount of additives in food simulant at the steady state, V_P is the polymer volume and V_F the food simulant volume, $(q_n)_n$, the positive roots of the equation $\tan q = -\alpha q$ and $K_{P,F}$, the partition coefficient of the additive in the polymer/food simulant system.

The numerical simulations were carried out using Matlab® software and its *lsqnonlin* function to estimate the D_{app}. To evaluate the correlation between experimental and estimated data, the percentage of the root mean-square error (% RMSE) was calculated using the following equation:

$$\text{RMSE} = \frac{1}{M_0}\sqrt{\frac{1}{N}\sum_{i=1}^{N}\left((M_t)_{\text{experimental}} - (M_t)_{\text{predicted}}\right)^2} \times 100 \quad (8)$$

Where: M_0 is the initial mass of additive in the biopolymer film and M_t is the mass of additive in the food simulant at time t.

2.12.2 Piringer correlation

The Piringer correlation (1994) estimates the worst case additive diffusivity in a given polymer by correlating the diffusion coefficient with the molar mass of additives and the temperature. D_P (Eq. 9) can be refined to not depend on experimental data (Brandsch et al., 2002).

$$D_P = D_0 \exp\left[A_P - 0.1351\,M^{\frac{2}{3}} + 0.003\,M - \frac{10454}{T}\right] \quad (9)$$

With: $D_0 = 10^4$ cm².s^{-1} = 1 m².s^{-1} and $A_P = A'_P - \frac{\tau}{T}$

Where the parameter A_P is linked to the polymer and describes the basic diffusion behavior of the polymer matrix in relation to the migrants, M is the molar mass of the additive, T is the absolute temperature and τ is a polymer specific "activation temperature" increment. The apostrophe ' indicates the parameter is temperature independent.

The parameters A'_P and τ are given in Table 2 (Begley et al., 2005). In the absence of specific parameters for PBSA and PHBV, those for LDPE and PET were used for, respectively, low and high barrier property polymers.

3 Results and discussion

3.1 Microstructure of composite material

Because the interaction between polymers and nanoclays determines the formation of exfoliated nanocomposite materials, clay modification has been extensively studied (Muñoz-Shugulí et al., 2019). Exfoliated nanoparticles reduce diffusion by creating tortuosity effect and results in higher transfer properties (Nasiri et al. 2016).

The degree of exfoliation of nanoclay platelets in biopolymer matrices was measured by XRD (Fig. 1 A) and TEM (Fig. 1 B). As expected, the analysis of the C-30B powder by XRD revealed a diffraction peak at 4.9°, corresponding to an interlayer spacing of 1.8 nm (Bharadwaj et al., 2002). The analysis of neat biopolymers exhibited no diffraction peaks in the studied 2Θ angle range, while the analysis of nanocomposites revealed one diffraction peak with a shift towards the smallest angles compared to C-30B powder, 2.7° for PBSA NCP and 2.2° for PHBV NCP, which respectively corresponds to a d-spacing of 3.3 nm and 4.0 nm. Similar values were reported for PBSA NCP (Charlon et al., 2015a) and PHBV NCP (Bordes et al., 2008). This increase in the interlayer distance reflects the formation of intercalated structures, confirmed by TEM observations which indicated both intercalated and exfoliated structures for nanocomposite materials.

279 ### 3.2 Migration curves of additives from studied films into food simulants

280 The desorption kinetic of each additive from polymers into food simulants was measured
281 over time, until 10 days, or 30 days in the case of PHBV contaminated with high molar mass
282 additives. An example of desorption kinetics is reported in Fig. 2, for methyl stearate additive,
283 from neat and nanocomposite PBSA into 95% ethanol food simulant.

284 For all molecules, a good correlation was observed between migration experimental data
285 and simulated curves using Eq. (6), with a RMSE inferior to 6%, calculated using Eq. (8).

286 Desorption curves can be analyzed in their growth phase, from which the diffusion
287 coefficient can be estimated, and in their state of equilibrium, from which the partition
288 coefficient can be estimated. The addition of nanoclays in the polymer matrix has varying
289 effects on both phases according to the nature of the diffusing additives (Nasiri et al. 2016).

290 ### 3.3 Comparison of the D_{app} of additives in neat and nanocomposites materials

291 The estimation of the D_{app} of each additive from biopolymer into food simulant is reported
292 in Fig. 3, with the respective impacts of: polymer type, food simulant, and the effect of
293 nanoparticle incorporation.

294 The differences in the D_{app} in the various systems, illustrated by the differing scales of
295 the histograms, reflect the influences of the polymer type and the food simulant in contact. As
296 in previous works that highlight the poor gas barrier properties of PBSA (Phua et al., 2013), the
297 diffusivity values measured in PBSA are between five and twenty times lower than those in
298 PHBV, which normally has good barrier properties (Crétois et al., 2014).

299 Contact with 95% ethanol seems to have a dramatic impact: producing diffusion values
300 nearly ten times higher than for iso-octane contact. The very peculiar behavior of polyesters in
301 contact with ethanol was already reported for PET (Begley and Hollifield, 1990), PLA
302 (Jamshidian et al., 2012), and PHBV (Chea et al., 2015).

For PBSA and PHBV matrices with nanoparticles in contact with 95% ethanol and iso-octane, the D_{app} varies according to additives. The impact of nanoparticles is not significant if compared to the impact of the biopolymer type or food simulant in contact. For PBSA in contact with 95% ethanol, nanoparticles decreased the D_{app} for all additives. In contact with iso-octane, nanoparticles increased the D_{app}, especially for low molar mass additives. For PHBV, nanoparticles increased the D_{app} significantly whatever the food simulant in contact.

These results contradict previous conclusions on conventional synthetic materials. For polyurethane, there is a negative correlation between C-30B (concentrations 0 - 50 wt%) and the diffusivity of three volatile organic compounds: toluene, decane, and butanol (Herrera-Alonso et al., 2009). Nasiri et al. (2016) measured the diffusivities in LLDPE with a wide range of additives exposed to four food simulants: D_{app} decreased with the addition of Cloisite regardless of the nature of the diffusing substance. Therefore, whereas plastic-based nanocomposite materials meet inertia criteria regarding the migration of low molar mass substances, the behavior of biodegradable materials raises new concerns relating to compliance with regulations and consumer safety. Given the limited available data, it is difficult to establish behavioral laws to describe the specific impact of nanoclays on the evolution of the D_{app} of low molar mass additives. In addition to the tortuosity effect demonstrated in section 3.1, these results suggest that nanoparticles modify polymer structures (size, shape, or arrangement of spherulites, and degree of crystallinity) and thus their transfer properties.

3.4 Predicting the D_{app} of additives according to molar mass

The D_{app} of additives is related to their specific volume and, consequently, to their molar mass: $D \sim M^{-\alpha}$ with a scaling parameter α that can be related to the transport mechanism (Lodge, 1999).

Fig. 4, below, shows the D_{app} of additives in function of their molar mass in neat and nanocomposite PBSA (Fig. 4 A) and PHBV (Fig. 4 B) in contact with 95% ethanol and iso-octane food simulants. The linear dependence of Log (D) = f (M) is clearer for PBSA than PHBV. The dependence of the diffusion coefficient on size has already been demonstrated in natural rubber and in a glassy synthetic polymer (Chern et al. 1985; Reynier et al. 2001; Martinez-Lopez et al., 2016). The inclusion of nanoparticles does not contradict this relationship given their weak influence on additive diffusivity.

Log D being correlated with the molar mass of additives, a Piringer correlation can be applied to PBSA and PHBV biopolyesters. This empirical model would enable verification of accordance with European regulations of suitability for food contact of materials on the basis of an overestimation of the diffusion coefficient of plastic additives.

Lacking the specific parameters, A'_p and τ, for PBSA and PHBV, the regression was performed using the values for LDPE and PET, these two polymers being selected as references for their low and high barrier properties respectively (Arora and Padua, 2010). The curves obtained from the Piringer model using key parameters of LDPE and PET are presented in Fig. 4. Migration modelling can provide the upper migration values, necessary to predict a reliable worst-case scenario for bio-polyesters. While the PET Piringer model underestimates the diffusivity values measured of bio-polyesters, the LDPE model is better adapted, slightly overestimating diffusivity (except for high molar mass additives), especially for neat and nanocomposite PBSA in contact with 95% ethanol. The values of A'_p and τ, although based on the integration of large quantities of experimental data are insufficient to provide Piringer parameters guaranteeing systematic overestimation of migration levels from PHBV and PBSA based packaging. However, the results of this study suggest that the incorporation of nanoclay does not modify these recommendations.

3.5 Impact of the sorption of food simulant

The contact of polymers with food simulating liquids can modify their transport properties (Figge, 1972), and the presence of nanoparticles is likely to impact these interactions. The sorption of food simulant by the semi-crystalline biopolymer usually induces swelling in the biopolymer, which accelerates additive migration and increases the diffusion coefficient value (Reynier et al., 2001; Barnes et al., 2007).

The solvent uptake of PBSA, PHBV and their corresponding nanocomposites after 10 days of contact with 95% ethanol and iso-octane at 40°C were summarized in Table 3. The sorption of ethanol by both tested packaging films could explain the high D_{app} values measured during the contact with this food simulant (Fig. 3).

In the case of PBSA based materials, significant ethanol uptakes of 3.5% (neat) and 4.7% (nanocomposite) were recorded, although there was no measurable change in film thickness. The 95% ethanol sorption value of PHBV is in accordance with the value reported by Chea et al. (2015) on the same matrix/food simulant system. As mentioned in section 3.3, the peculiar interaction of 95% ethanol with polyesters was already proven with PET (Begley and Hollifield, 1990; Widén et al., 2004; Kim and Lee, 2012), PLA (Jamshidian et al., 2012) and PHBV (Chea et al., 2015).

For neat and nanocomposite PBSA in contact with iso-octane, no solvent uptake was detected. Neat and nanocomposite PHBV in contact with iso-octane had a $< 1.5\%$, solvent uptake.

The incorporation of nanoclays in the polymer matrix leads to different behaviors depending on the nature of the food simulant. 95% ethanol uptake increased with nanoclays whatever the polymer. In PHBV, addition of nanoclay reduced iso-octane uptake. Nanoclays are hydrophilic and therefore soluble in ethanol (Ho and Glinka, 2003) which leads to a greater

375 solvent uptake. However, we cannot attribute the increase in D_{app} values observed for all
376 additives solely to solvent sorption.

377 **3.6 Impact of the semi-crystalline structure of bio-nanocomposites**

378 Bio-nanocomposite transfer properties are influenced by factors such as the degree of
379 crystallinity of the polymer: high crystallinity limits movement and therefore limits the
380 diffusion of migrating substances (Hedenqvist et al., 1996).

381 The degrees of crystallinity of neat and nanocomposite biopolymers evaluated by DSC
382 experiments on films without contact and after 10 days in contact with food simulants at 40°C
383 were summarized in Table 4.

384 PHBV has a high degree of crystallinity (Chea et al., 2015): almost twice that of PBSA,
385 which may explain the difference between D_{app} values for these two materials.

386 The degree of crystallinity of polymers proved to be food simulant dependent. In contact
387 with 95% ethanol, the degree of crystallinity decreases by 1.3% for PHBV, and by 3.9% for
388 PBSA. These results are similar to previous research conducted on these polymers and food
389 simulants (Chea et al., 2015; Siracusa et al., 2015). The decrease in crystallinity could be
390 attributed to the degradation of polymer chains due to hydrolysis reactions induced by the 95%
391 ethanol. However, in contact with iso-octane, there was no change in the degree of crystallinity
392 for PHBV, a 1.3% increase for PHBV NCP and a close to 2% increase for neat and
393 nanocomposite PBSA. This result confirms the findings of Chea et al. (2015): there was no
394 structural change to PHBV in contact with iso-octane.

395 C-30B decreases the degree of crystallinity of the two polymers by nearly 10%. This
396 has previously been observed for PBSA/C30B (Sinha Ray et al., 2005), and for PHBV/OMMT
397 (Wang et al., 2005). It can be explained by the full exfoliation of nanoclays platelets in the
398 polymer matrix (see section 3.1), which restricts the mobility of the polymer chains and thus
399 prevents them from crystallizing (Krikorian and Pochan, 2003). This decrease results in an

400 increase of the amorphous phase in which the diffusivity of additives is facilitated, this tendency
401 is observed in all cases apart from PBSA in 95% ethanol (Fig. 3).

402 Although the degree of crystallinity of materials is known to impact the transport
403 properties of semi-crystalline polymers, strict correlation between crystallinity and diffusivity
404 cannot be concluded in the case of biodegradable packaging materials. For instance, D_{app} of
405 additives in PBSA are three times higher in contact with 95% ethanol than with iso-octane, but
406 the crystallinity of both materials is similar. The relationship between diffusion and crystallinity
407 on a macroscopic scale remains obscure. Nanoclays generate localized crystalline gradients
408 (Wurm et al., 2010) which could modify the transport properties of materials.

409 ## 4 Conclusion

410 The incorporation of nanoclays in biodegradable materials raises new questions related
411 to their food contact suitability. While the few studies carried out on synthetic plastic materials
412 agree that the inclusion of nanoclays decreases diffusivity, this work demonstrates that this is
413 not the case for biodegradable materials. The presence of nanoparticles affects diffusion
414 variously, depending on the nature of the migrating substance and particularly depending on
415 the nature of the food simulant. As previously observed for biopolyester based materials,
416 contact with ethanol, whose diffusion activation mechanisms remain unclear, is the worst-case
417 scenario. This particular sensitivity of biopolyesters to ethanol, especially when they
418 incorporate inorganic nanoparticles such as nanoclays, underscores the problem of applying
419 existing recommended testing conditions for the evaluation of conventional plastic materials to
420 these new materials. Ethanol sorption, which promotes the crystallization of synthetic
421 polyesters and thus prevents the mobility of low molecular weight molecules, appears to be
422 enhanced by the incorporation of clay nanoparticles. Being necessarily cautious we cannot, with
423 sufficient accuracy, predict migration levels from bio-nanocomposite packaging using diffusion
424 models generally applied to food contact material considered as continuous homogeneous

phase. However, Piringer's empirical model remains an applicable way to overestimate migration and guarantee consumer safety. This model would be more effective with the creation and inclusion of database of the diffusion coefficients of low molecular weight molecules in these materials.

Funding

This work has been carried out in the framework of the Labex SERENADE (ANR-11-LABX-0064) funded by the « Investissements d'Avenir » French Government program managed by the French National Research Agency (ANR).

Compliance with ethical standards

The authors declare that there is no conflict of interest regarding the publication of this paper.

References

Aguzzi, C., Cerezo, P., Viseras, C., Caramella, C., 2007. Use of clays as drug delivery systems: possibilities and limitations. Appl. Clay Sci. 36, 22–36. https://doi.org/10.1016/j.clay.2006.06.015

Arora, A., Padua, G.W., 2010. Review: nanocomposites in food packaging, Journal of Food Science. https://doi.org/10.1111/j.1750-3841.2009.01456.x

Barham, P.J., Keller, A., Otun, E.L., 1984. Crystallization and morphology of a bacterial thermoplastic: poly-3-hydroxybutyrate. J. Mater. Sci. 19, 2781–2794.

Barnes, K.A., Sinclair, C.R., Watson, D.H., 2007. Chemical migration and food contact materials.

Begley, T.H., Castle, L., Feigenbaum, A., Franz, R., Hinrichs, K., Lickly, T., Mercea, P., Milana, M., O'Brien, A., Rebre, S., Rijk, R., Piringer, O., 2005. Evaluation of migration models that might be used in support of regulations for food-contact plastics. Food Addit. Contam. 22, 73–90. https://doi.org/10.1080/02652030400028035

450 Begley, T.H., Hollifield, H.C., 1990. High-performance liquid chromatographic determination
451 of migrating poly(ethylene terephthalate) oligomers in corn oil. J. Agric. Food Chem. 38,
452 145–148.
453 Bharadwaj, R.K., Mehrabi, A.R., Hamilton, C., Trujillo, C., Murga, M., Fan, R., Chavira, A.,
454 Thompson, A.K., 2002. Structure - property relationships in cross-linked polyester - clay
455 nanocomposites. Polymer (Guildf). 43, 3699–3705.
456 Bordes, P., Pollet, E., Bourbigot, S., Avérous, L., 2008. Structure and properties of PHA/clay
457 nano-biocomposites prepared by melt intercalation. Macromol. Chem. Phys. 209, 1474–
458 1484. https://doi.org/10.1002/macp.200800022
459 Brandsch, J., Mercea, P., Rüter, M., Tosa, V., Piringer, O., 2002. Migration modelling as a tool
460 for quality assurance of food packaging Migration modelling as a tool for quality assurance
461 of food. Food Addit. Contam. 19, 29–41. https://doi.org/10.1080/0265203011005819
462 Carli, L.N., Crespo, J.S., Mauler, R.S., 2011. PHBV nanocomposites based on organomodified
463 montmorillonite and halloysite: the effect of clay type on the morphology and thermal and
464 mechanical properties. Compos. Part A Appl. Sci. Manuf. 42, 1601–1608.
465 https://doi.org/10.1016/j.compositesa.2011.07.007
466 Charlon, S., Follain, N., Chappey, C., Dargent, E., Soulestin, J., Sclavons, M., Marais, S., 2015.
467 Improvement of barrier properties of bio-based polyester nanocomposite membranes by
468 water-assisted extrusion. J. Memb. Sci. 496, 185–198.
469 https://doi.org/10.1016/j.memsci.2015.08.043
470 Charlon, S., Marais, S., Dargent, E., Soulestin, J., Sclavons, M., Follain, N., 2015. Structure–
471 barrier property relationship of biodegradable poly(butylene succinate) and poly[(butylene
472 succinate)-co-(butylene adipate)] nanocomposites: influence of the rigid amorphous
473 fraction. Phys. Chem. Chem. Phys. https://doi.org/10.1039/C5CP04969E
474 Chea, V., Angellier-Coussy, H., Peyron, S., Kemmer, D., Gontard, N., 2015. Poly(3-

475 hydroxybutyrate-co-3-hydroxyvalerate) films for food packaging: physical-chemical and
476 structural stability under food contact conditions. J. Appl. Polym. Sci. 133, 1–8.
477 https://doi.org/10.1002/app.41850
478 Chern, R.T., Koros, W.J., Hopfenberg, H.B., Stannett, V.T., 1985. Material selection for
479 membrane-based gas separations, in: Materials Science of Synthetic Membranes. pp. 25–
480 46.
481 Commission, E., 2011. COMMISSION REGULATION (EU) No 10/2011 of 14 January 2011
482 on plastic materials and articles intended to come into contact with food.
483 Crank, J., 1975. The mathematics of diffusion. Oxford.
484 Crétois, R., Follain, N., Dargent, E., Soulestin, J., Bourbigot, S., Marais, S., Lebrun, L., 2014.
485 Microstructure and barrier properties of PHBV/organoclays bionanocomposites. J. Memb.
486 Sci. 467, 56–66. https://doi.org/10.1016/j.memsci.2014.05.015
487 Duncan, T. V., 2011. Applications of nanotechnology in food packaging and food safety:
488 Barrier materials, antimicrobials and sensors. J. Colloid Interface Sci. 363, 1–24.
489 https://doi.org/10.1016/j.jcis.2011.07.017
490 European Food Safety Authority, 2011. Scientific opinion on the criteria to be used for safety
491 evaluation of a mechanical recycling process to produce recycled PET intended to be used
492 for manufacture of materials and articles in contact with food.
493 https://doi.org/10.2903/j.efsa.2011.2184.Available
494 Farhoodi, M., Mohammadifar, M.A., Mousavi, M., Sotudeh-Gharebagh, R., Emam-Djomeh,
495 Z., 2016. Migration kinetics of ethylene glycol monomer from PET bottles into acidic food
496 simulant: effects of nanoparticle presence and matrix morphology. J. Food Process Eng.
497 1–8. https://doi.org/10.1111/jfpe.12383
498 Figge, K., 1980. Migration of components from plastics-packaging materials into packed goods
499 - test methods and diffusion models. Prog. Polym. Sci. 6, 187–252.

500 Figge, K., 1972. Migration of additives from plastics films into edible oils and fat simulants.
501 Food Cosmet. Toxicol. 10, 815–828.
502 Food and Drug Administration, 2006. Guidance for industry: use of recycled plastics in food
503 packaging (chemistry considerations).
504 Hedenqvist, M., Angelstok, A., Edsberg, L., Larssont, P.T., Gedde, U.W., 1996. Diffusion of
505 small-molecule penetrants in polyethylene: free volume and morphology. Polymer
506 (Guildf). 37, 2887–2902.
507 Helmroth, I.. E., Bekhuis, H.A.M., Linssen, J.P.H., Dekker, M., 2002. Direct measurement of
508 additive migration from low-density polyethylene as a function of space and time. J. Appl.
509 Polym. Sci. 86, 3185–3190. https://doi.org/10.1002/app.11324
510 Herrera-Alonso, J.M., Marand, E., Little, J., Cox, S.S., 2009. Polymer/clay nanocomposites as
511 VOC barrier materials and coatings. Polymer (Guildf). 50, 5744–5748.
512 https://doi.org/10.1016/j.polymer.2009.09.054
513 Ho, D.L., Glinka, C.J., 2003. Effects of solvent solubility parameters on organoclay dispersions.
514 Chem. Mater. 1309–1312.
515 Hongsriphan, N., Pinpueng, A., 2019. Properties of agricultural films prepared from
516 biodegradable poly(butylene succinate) adding natural sorbent and fertilizer. J. Polym.
517 Environ. 27, 434–443. https://doi.org/10.1007/s10924-018-1358-5
518 Iggui, K., Le Moigne, N., Kaci, M., Cambe, S., Degorce-Dumas, J.-R., Bergeret, A., 2015. A
519 biodegradation study of poly(3-hydroxybutyrate-co-3-hydroxyvalerate)/organoclay
520 nanocomposites in various environmental conditions. Polym. Degrad. Stab. 119, 77–86.
521 https://doi.org/10.1016/j.polymdegradstab.2015.05.002
522 Jamshidian, M., Tehrany, E.A., Desobry, S., 2012. Release of synthetic phenolic antioxidants
523 from extruded poly lactic acid (PLA) film. Food Control 28, 445–455.
524 https://doi.org/10.1016/j.foodcont.2012.05.005

525 Ke, Y., Long, C., Qi, Z., 1999. Crystallization, properties, and crystal and nanoscale
526 morphology of PET-clay nanocomposites. J. Appl. Polym. Sci. 71, 1139–1146.
527 Kim, D.-J., Lee, K.T., 2012. Analysis of specific migration of monomers and oligomers from
528 polyethylene terephthalate bottles and trays according to the testing methods as prescribed
529 in the legislation of the EU and Asian countries. Polym. Test. 31, 1001–1007.
530 https://doi.org/10.1016/j.polymertesting.2012.07.012
531 Kirwan, M.J., Strawbridge, J.W., 2003. Plastics in food packaging, in: Food Packaging
532 Technology. pp. 174–240.
533 Krikorian, V., Pochan, D.J., 2003. Poly(L-Lactic Acid)/layered silicate nanocomposite:
534 fabrication, characterization, and properties. Chem. Mater. 15, 4317–4324.
535 Lodge, T.P., 1999. Reconciliation of the molecular weight dependence of diffusion and
536 viscosity in entangled polymers. Phys. Rev. Lett. 83, 3218–3221.
537 Mauricio Iglesias, M., 2009. Impact of high pressure thermal treatments on food/packaging
538 interactions. Montpellier.
539 Muñoz-Shugulí, C., Rodríguez, F.J., Bruna, J.E., Galotto, M.J., Sarantópoulos, C., Favaro
540 Perez, M.A., Padula, M., 2019. Cetylpyridinium bromide-modified montmorillonite as
541 filler in low density polyethylene nanocomposite films. Appl. Clay Sci. 168, 203–210.
542 https://doi.org/10.1016/j.clay.2018.10.020
543 Nasiri, A., Gontard, N., Gastaldi, E., Peyron, S., 2017. Contribution of nanoclay to the additive
544 partitioning in polymers. Appl. Clay Sci. 146, 27–34.
545 https://doi.org/10.1016/j.clay.2017.05.024
546 Nasiri, A., Peyron, S., Gastaldi, E., Gontard, N., 2016. Effect of nanoclay on the transfer
547 properties of immanent additives in food packages. J. Mater. Sci. 51.
548 https://doi.org/10.1007/s10853-016-0208-x
549 Nikolic, M.S., Djonlagic, J., 2001. Synthesis and characterization of biodegradable

poly(butylene succinate-co-butylene adipate)s. Polym. Degrad. Stab. 74, 263–270.

Otero-Pazos, P., Pereira de Abreu, D.A., Sendon, R., Rodriguez Bernaldo de Quiros, A., Angulo, I., Cruz, J.M., Paseiro-Losada, P., 2016. Determination of partition coefficients of selected model migrants between polyethylene and polypropylene and nanocomposite polypropylene. J. Chem. 1–10.

Paul, D.R., Robeson, L.M., 2008. Polymer nanotechnology: nanocomposites. Polymer (Guildf). 49, 3187–3204. https://doi.org/10.1016/j.polymer.2008.04.017

Pereira de Abreu, D.A., Cruz, J.M., Angulo, I., Paseiro Losada, P., 2010. Mass transport studies of different additives in polyamide and exfoliated nanocomposite polyamide films for food industry. Packag. Technol. Sci. 23, 59–68. https://doi.org/10.1002/pts

Perumal, A.B., Sellamuthu, P.S., Nambiar, R.B., Sadiku, E.R., Phiri, G., Jayaramudu, J., 2018. Effects of multiscale rice straw (Oryza sativa) as reinforcing filler in montmorillonite-polyvinyl alcohol biocomposite packaging film for enhancing the storability of postharvest mango fruit (Mangifera indica L.) 158, 1–10. https://doi.org/10.1016/j.clay.2018.03.008

Phua, Y.J., Chow, W.S., Mohd Ishak, Z.A., 2013. Organomodification of montmorillonite and its effects on the properties of poly(butylene succinate) nanocomposites. Polym. Eng. Sci. 53, 1947–1957. https://doi.org/10.1002/pen

Piringer, O., 1994. Evaluation of plastics for food packaging. Food Addit. Contam. 11, 221–230.

Rajan, K.P., Thomas, S.P., Gopanna, A., Chavali, M., 2018. Polyhydroxybutyrate (PHB): a standout biopolymer for environmental sustainability, in: Handbook of Ecomaterials. pp. 1–23.

Reynier, A., Dole, P., Feigenbaum, A., 2001a. Additive diffusion coefficients in polyolefins. II. Effect of swelling and temperature on the D = f (M) correlation. J. Appl. Polym. Sci. 82, 2434–2443. https://doi.org/10.1002/app.2094

575 Reynier, A., Dole, P., Humbel, S., Feigenbaum, A., 2001b. Diffusion coefficients of additives
576 in polymers . I. Correlation with geometric parameters. J. Appl. Polym. Sci. 82, 2422–
577 2433. https://doi.org/10.1002/app.2093
578 Šimon, P., Chaudhry, Q., Bakoš, D., 2008. Migration of engineered nanoparticles from polymer
579 packaging to food – a physicochemical view. J. Food Nutr. Res. 47, 105–113.
580 Sinha Ray, S., Bandyopadhyay, J., Bousmina, M., 2008. Influence of degree of intercalation on
581 the crystal growth kinetics of poly[(butylene succinate)-co-adipate] nanocomposites. Eur.
582 Polym. J. 44, 3133–3145. https://doi.org/10.1016/j.eurpolymj.2008.07.035
583 Sinha Ray, S., Bousmina, M., Okamoto, K., 2005. Structure and properties of nanocomposites
584 based on poly(butylene succinate-co-adipate) and organically modified montmorillonite.
585 Macromol. Mater. Eng. 290, 759–768. https://doi.org/10.1002/mame.200500203
586 Siracusa, V., Lotti, N., Munari, A., Dalla Rosa, M., 2015. Poly(butylene succinate) and
587 poly(butylene succinate-co-adipate) for food packaging applications: gas barrier
588 properties after stressed treatments. Polym. Degrad. Stab. 119, 35–45.
589 https://doi.org/10.1016/j.polymdegradstab.2015.04.026
590 Sorrentino, A., Gorrasi, G., Vittoria, V., 2007. Potential perspectives of bio-nanocomposites for
591 food packaging applications. Trends Food Sci. Technol. 18, 84–95.
592 https://doi.org/10.1016/j.tifs.2006.09.004
593 Tenn, N., Follain, N., Soulestin, J., Crétois, R., Bourbigot, S., Marais, S., 2013. Effect of
594 nanoclay hydration on barrier properties of PLA/montmorillonite based nanocomposites.
595 J. Phys. Chem. 117, 12117–12135.
596 Tharanathan, R.N., 2003. Biodegradable films and composite coatings: past, present and future.
597 Trends Food Sci. Technol. 14, 71–78. https://doi.org/10.1016/S0924-2244(02)00280-7
598 Wang, S., Song, C., Chen, G., Guo, T., Liu, J., Zhang, B., Takeuchi, S., 2005. Characteristics
599 and biodegradation properties of poly(3-hydroxybutyrate-co-3-

600 hydroxyvalerate)/organophilic montmorillonite (PHBV/OMMT) nanocomposite. Polym.
601 Degrad. Stab. 87, 69–76. https://doi.org/10.1016/j.polymdegradstab.2004.07.008
602 Widén, H., Leufvén, A., Nielsen, T., 2004. Migration of model contaminants from PET bottles:
603 influence of temperature, food simulant and functional barrier. Food Addit. Contam. 21,
604 993–1006. https://doi.org/10.1080/02652030400009217
605 Wurm, A., Ismail, M., Kretzschmar, B., Pospiech, D., Schick, C., 2010. Retarded crystallization
606 in polyamide/layered silicates nanocomposites caused by an immobilized interphase.
607 Macromolecules 43, 1480–1487. https://doi.org/10.1021/ma902175r
608 Yuan, Q., Awate, S., Misra, R.D.K., 2006. Nonisothermal crystallization behavior of melt-
609 intercalated polyethylene-clay nanocomposites. J. Appl. Polym. Sci. 102, 3809–3818.
610 https://doi.org/10.1002/app.24852
611

(A) XRD spectra

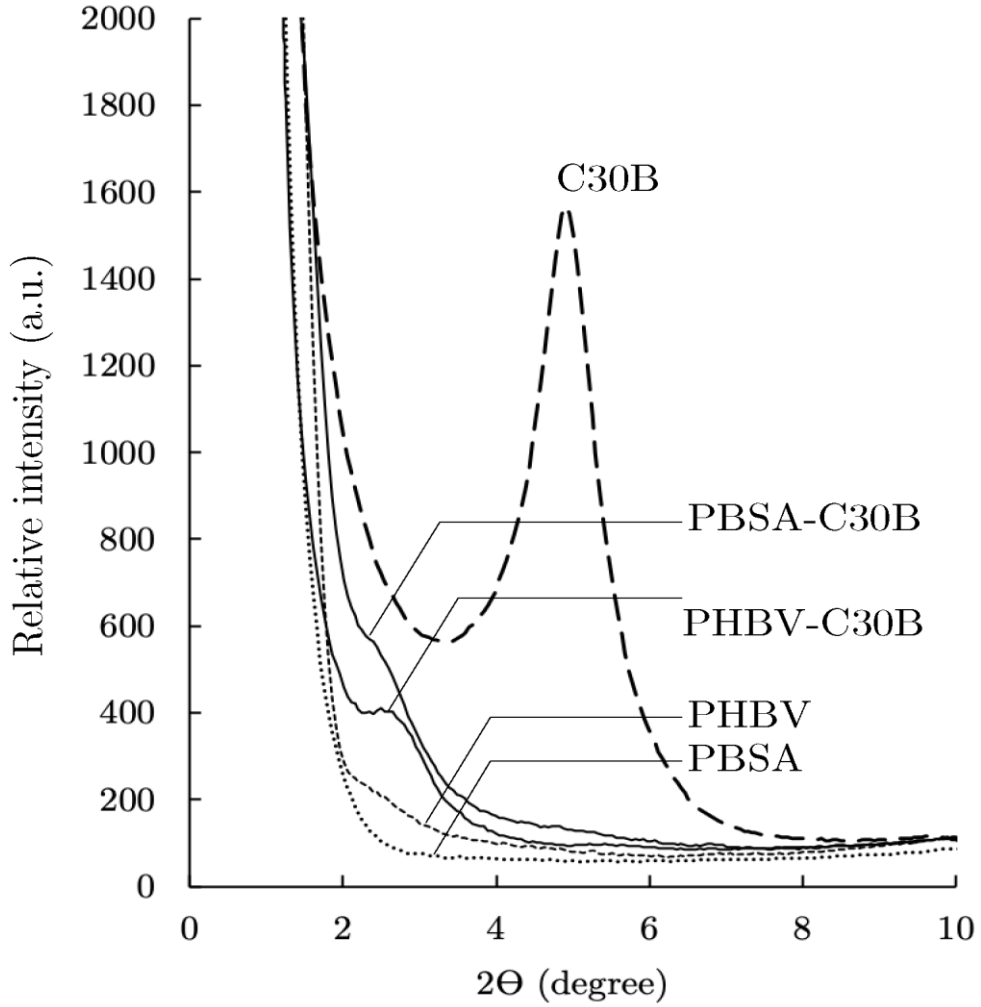

(B) TEM image

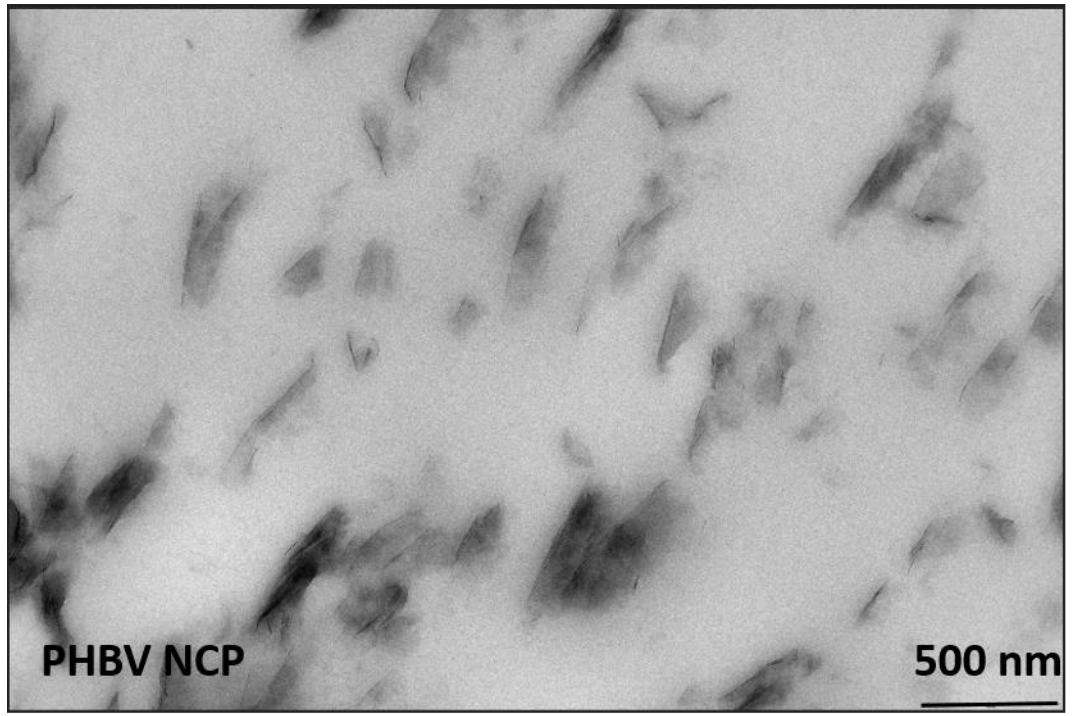

Fig. 1. XRD spectra of neat and nanocomposite polymers (A) and TEM image (B) of PHBV NCP.

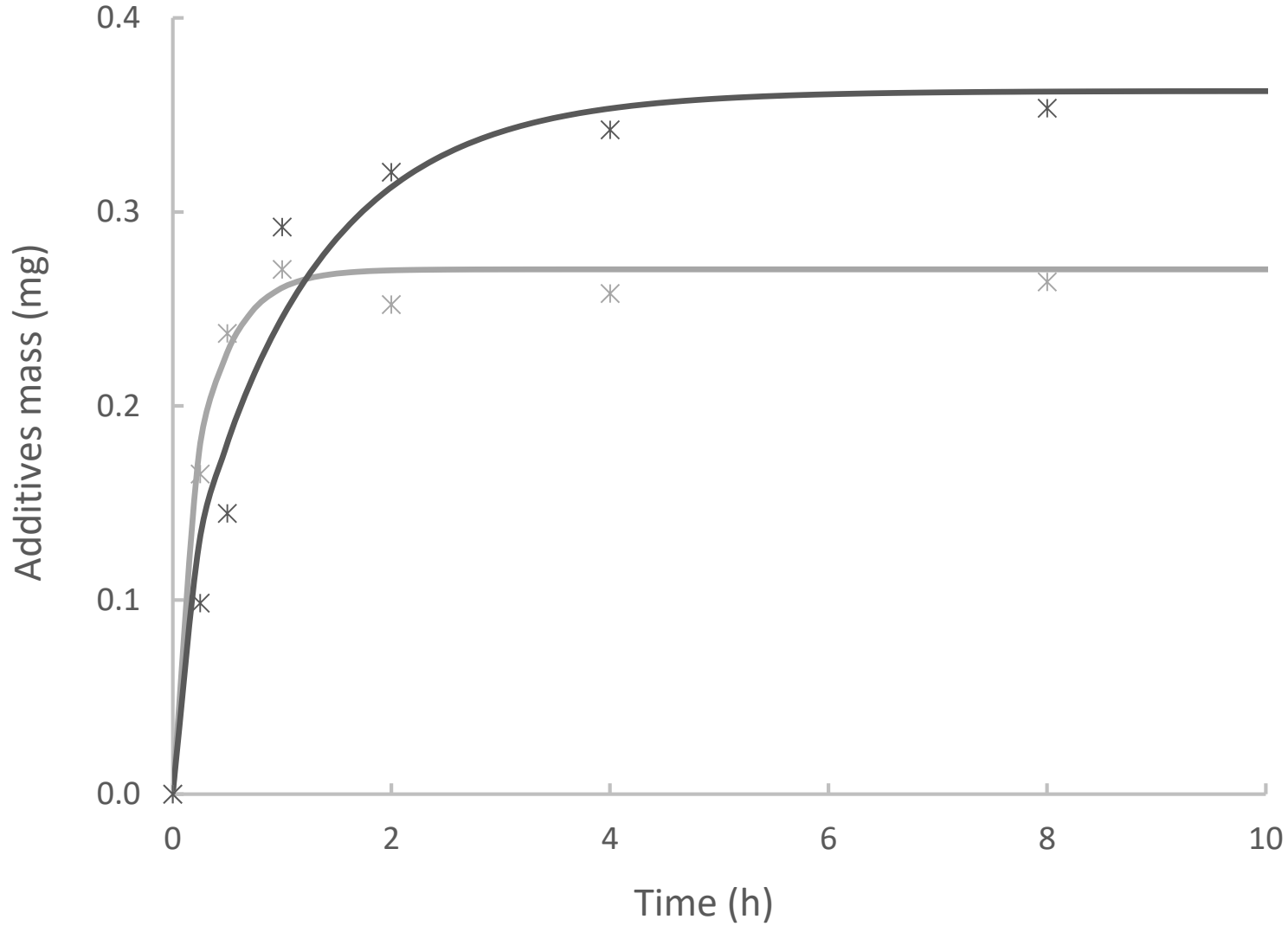

Fig. 2. Experimental (symbols) and simulated (curves) desorption kinetics for the first 10 hours for PBSA (grey) and PBSA NCP (black) into 95% ethanol for methyl stearate.

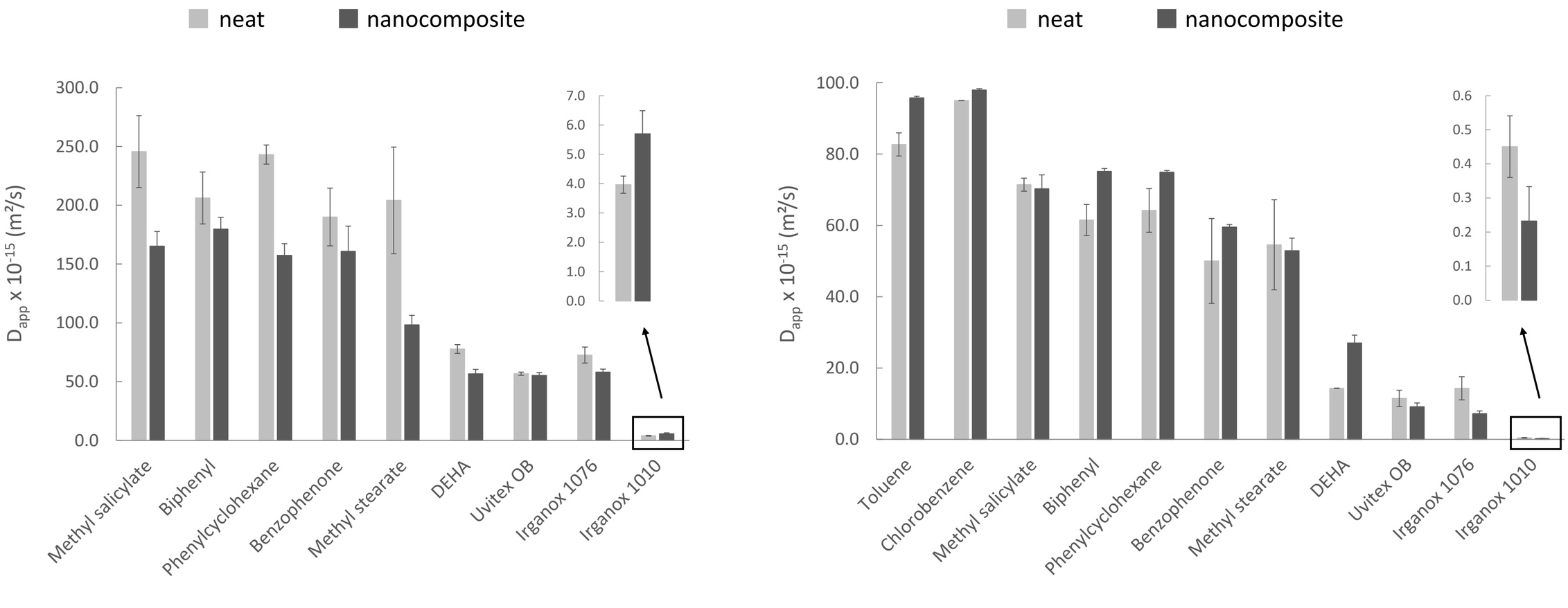

Fig. 3. Comparison of D_{app} of additives in neat (grey bars) and nanocomposite (black bars) PBSA (Fig. A and B) and PHBV (Fig. C and D) films in contact with food simulants: 95% ethanol (Fig. A and C) and iso-octane (Fig. B and D).

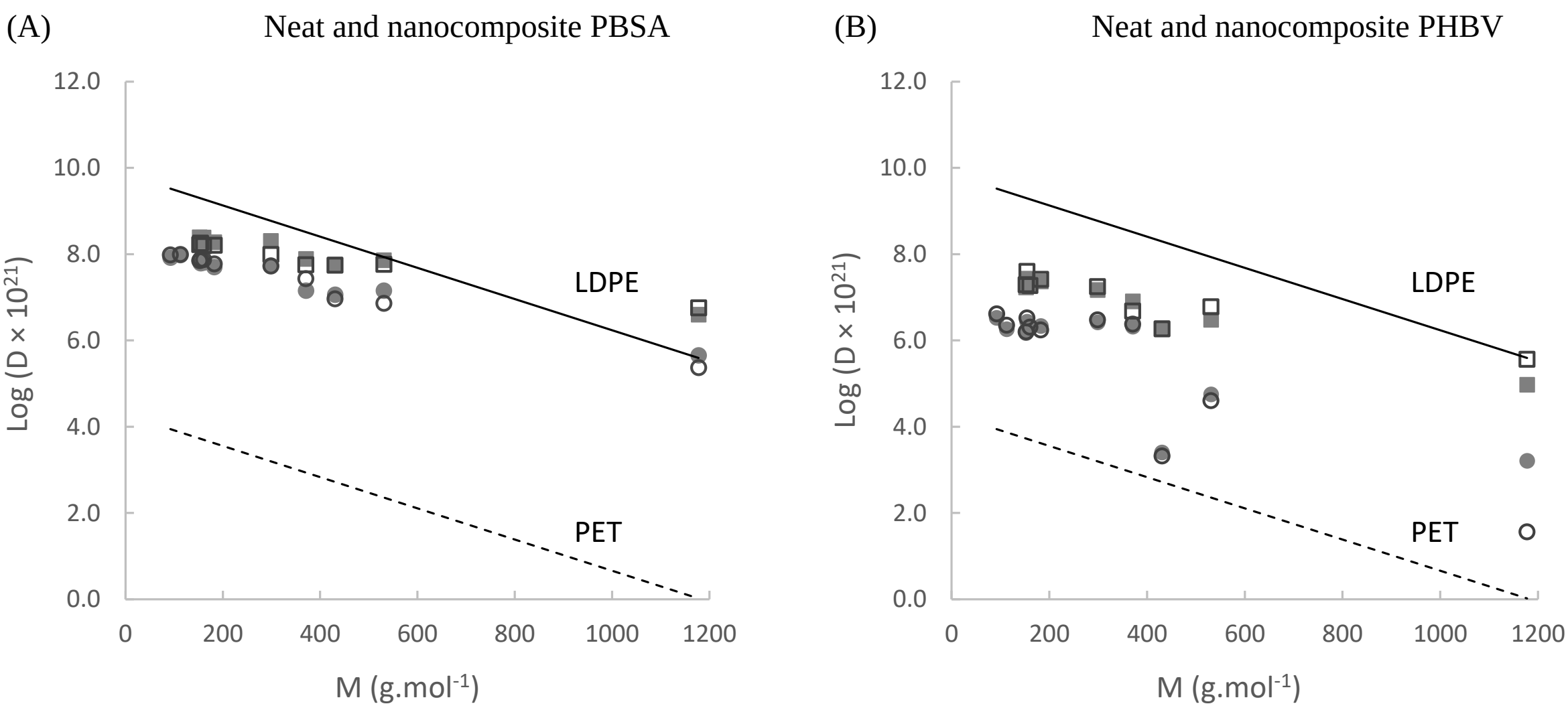

Fig. 4. D_{app} of additives in function of additives molar mass for neat and nanocomposite PBSA (A) and PHBV (B). Neat PBSA or PHBV in contact with 95% ethanol (■) or iso-octane (●) and PBSA NCP or PHBV NCP in contact with 95% ethanol (□) or iso-octane (○). Piringer estimations in LDPE (—) and PET (- - -) at 40°C.

Table 1: List of selected additives.

Category	Code	Physical properties	CAS number	M ($g.mol^{-1}$)
High molar mass contaminants	Uvitex OB	Non-volatile	7128-64-5	430.56
	Irganox 1076	Non-volatile polar	2082-79-3	530.86
	Irganox 1010	Non-volatile	6683-19-8	1177.63
Low molar mass contaminants	Toluene	Volatile non-polar	108-88-3	92.14
	Chlorobenzene	Volatile polar	108-90-7	112.56
	Methyl salicylate	Non-volatile polar	119-36-8	152.15
	Biphenyl	Volatile non-polar	92-52-4	154.21
	Phenyl cyclohexane	Non-volatile non-polar	827-52-1	160.26
	Benzophenone	Non-volatile polar	119-61-9	182.22
	Methyl stearate	Non-volatile non-polar	112-61-8	298.50
	DEHA	Non-volatile polar	103-23-1	370.57

Table 2: LDPE and PET specific parameters.

Polymer	A'_P	τ
LDPE	10	0
PET	2.2	1577

Table 3: Solvent uptake of films after 10 days of contact with food simulant at 40°C.

	Solvent uptake (%)	
Food simulant / Sample	95% ethanol	Iso-octane
PBSA	3.7 ± 0.5	0
PBSA NCP	4.7 ± 0.1	0
PHBV	3.5 ± 0.1	1.3 ± 0.1
PHBV NCP	3.8 ± 0.2	0.5 ± 0.1

Table 4: Degree of crystallinity of film samples without contact and after 10 days of contact with 95% ethanol or iso-octane at 40°C.

	Degree of crystallinity (X_C) (%)		
Sample	Without contact	95% ethanol	Iso-octane
PBSA	38.2 ± 0.0	36.7 ± 0.1	39.0 ± 0.1
PBSA NCP	34.9 ± 0.4	34.1 ± 0.3	35.7 ± 0.1
PHBV	62.8 ± 1.6	62.0 ± 0.1	62.9 ± 0.1
PHBV NCP	55.0 ± 0.4	53.6 ± 0.3	55.7 ± 0.1